Recursively Deflated PCG for mechanical problems

C. Vuik, T.B. Jönsthövel, M.B. van Gijzen

Delft University of Technology

Numerical Linear Algebra - Algorithms, Applications, and Training Delft, The Netherlands April 10-13, 2012

Introduction

problem from the work floor: material analysis

Iterative methods

overview existing solvers

deflation method

recursive deflation

Numerical experiment: real asphalt core

Questions and references

problem from the work floor: material analysis

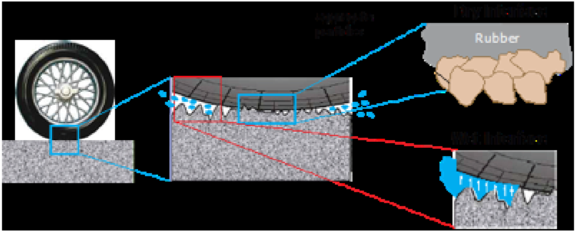

Figure: EU project, SKIDSAFE: asphalt-tire interaction

problem from the work floor: material analysis

20th century science

consider materials to be homogeneous

21th century science

shift from MACRO to MESO/MICRO scale

- Obtain CT scan from material specimen
- Convert CT scan to mesh
- Use finite element method for discretization of governing equations

problem from the work floor: material analysis

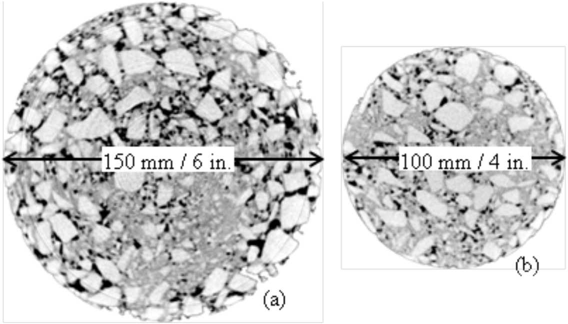

Figure: CT scan of asphalt column

problem from the work floor: material analysis

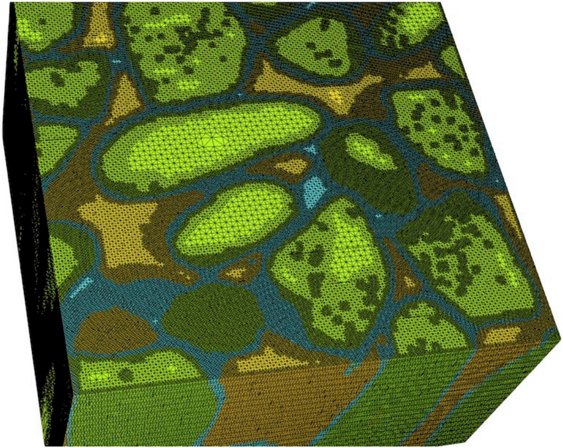

Figure: from CT scan to mesh, approx. 3 mln DOF

problem from the work floor: material analysis

governing equations

$$K\Delta u = \Delta f \tag{1}$$

Stiffness matrix K, change in displacement Δu and change of force Δf. The change of force involves evaluation of non-linear equations that depend on displacement field.

problem from the work floor: material analysis

properties of stiffness matrix K

- symmetric, positive definite: $\forall \Delta u \neq 0,\ \Delta u^T K \Delta u > 0$
- $K \in \mathbb{R}^{n \times n}$, $n >> 10^6$
- discontinuities in values matrix entries $\sim \mathcal{O}\left(10^6\right)$: ill-conditioned

Existing solvers

just some possible methods and pre conditioners

- preconditioned conjugate gradient method (PCG) combined with,
  - BIM: Jacobi, SSOR
  - Decomposition methods: (Additive-Schwarz) ILU(ϵ)
- direct solvers: MUMPS, PARDISO, SuperLU
- multigrid: geometric multigrid, algebraic multigrid (smoothed aggregation)

Existing solvers

bottom line: no free lunch

no black box solution for large, ill-conditioned systems

- performance of PCG depends on spectrum of K, large jumps induce small eigenvalues, hence performance degrades when number of jumps (different materials) increases
- direct solvers (may) become expensive for large meshes
- AMG can be insensitive to jumps, however to achieve this one has to define the coarse grid specifically

Use deflation

Deflation basedoperator is not a classical pre conditioner, i.e. it is not an approximation of K. The deflation operator is a projection which, by the right choice of the projection vectors, removes eigenvalues from the spectrum of the projected system.

definition

split displacement vector u,

$$u = \left(I - P^T\right) u + P^T u, \tag{2}$$

and let us define the projection P by,

$$P = I - KZ(Z^T KZ)^{-1} Z^T, \;\; Z \in \mathbb{R}^{n \times m} \tag{3}$$

the DPCG method

We use deflation based operator in conjunction with pre conditioning (e.g. diagonal scaling) to remove those small eigenvalues that correspond to the jumps (discontinuities) in the values of the stiffness matrix.

Deflated Pre conditioned Conjugate Gradient (DPCG) method

Solve for $M^{-1}PK\Delta u = M^{-1}P\Delta f$

How to choose the deflation vectors?

- We have observed in [2][1] that the rigid body modes of the regions corresponding to the different materials coincide with the eigenvectors of the 'jump' eigenvalues.
- By removing those rigid body modes (RBM) using deflation, we remove the corresponding 'jump' eigenvalues from the system.
- The rigid body modes of sets of finite elements can be easily computed.

[1] Jonsthovel et al., CMES, 2009

How do RBM relate to stiffness matrix K?

The kernel of the element matrix of an arbitrary unconstrained finite element is spanned by the rigid body modes of the element. In 3D six rigid body modes: three translations, three rotations.

How do RBM relate to stiffness matrix K?

Theorem

We assume a splitting $K = C + R$ such that C and R are symmetric positive semi-definite with $\mathcal{N}(C) = span\{Z\}$ the null space of C [1][2]. Then

$$\lambda_i(C) \leq \lambda_i(PK) \leq \lambda_i(C) + \lambda_{max}(PR). \tag{4}$$

Moreover, the effective condition number of PK is bounded by,

$$\kappa_{eff}(PK) \leq \frac{\lambda_n(K)}{\lambda_{m+1}(C)}. \tag{5}$$

[2] Vuik, Frank, SIAM, 2001

How do RBM relate to stiffness matrix K?

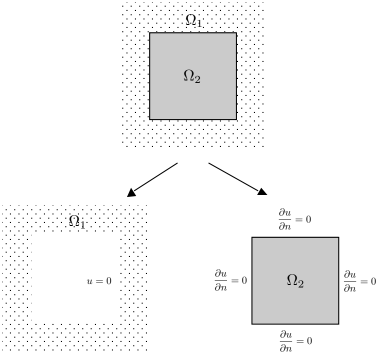

Figure: Principle of rigid body mode deflation

How do RBM relate to stiffness matrix K?

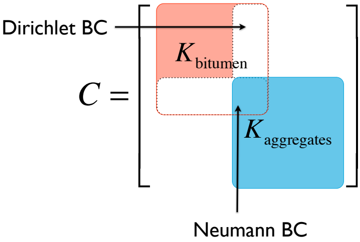

Figure: Principle of rigid body mode deflation: construction of C

How do RBM relate to stiffness matrix K?

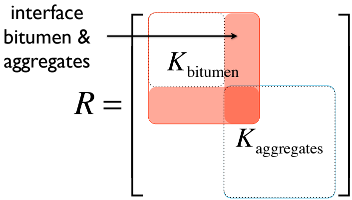

Figure: Principle of rigid body mode deflation: construction of R

Recursive deflation

However, the definition of P given by first theorem does not provide insight in the effect of individual deflation vectors on the spectrum of PK. Introduce a recursive deflation operator which can be used for more extensive eigenvalue analysis of PK.

Definition

$P^{(k)} = I - KZ_k(Z_k^{\mathrm{T}}KZ_k)^{-1}Z_k^{\mathrm{T}}$ with $Z_k = [\tilde{Z}_1, \tilde{Z}_2, ..., \tilde{Z}_k]$, where $\tilde{Z}_j \in \mathbb{R}^{n \times l_j}$ and has rank l_j.

Recursive deflation

Theorem

Let $P^{(k)}$ and Z_k as in Definition 2, then $P^{(k)}K = P_k P_{k-1} \cdots P_1 K$ where $P_{i+1} = I - \tilde{K}_i \tilde{Z}_{i+1} (\tilde{Z}_{i+1}^{\mathrm{T}} \tilde{K}_i \tilde{Z}_{i+1})^{-1} \tilde{Z}_{i+1}^{\mathrm{T}}$, $\tilde{K}_i = P_i \tilde{K}_{i-1}$, $\tilde{K}_1 = P_1 K$, $\tilde{K}_0 = K$, $\tilde{Z}_i^{\mathrm{T}} \tilde{K}_{i-1} \tilde{Z}_i^{\mathrm{T}}$ and $Z_i^{\mathrm{T}} K Z_i$ are non-singular because Z_i are of full rank and K is a symmetric positive definite matrix.

Recursive deflation

Proof.

by induction,

i. show $P_1 K = P^{(1)} K$ where $Z_1 = \tilde{Z}_1 \in \mathbb{R}^{n \times l_1}$,

ii. assume $P_{i-1}\tilde{K}_{i-2} = \tilde{K}_{i-1} = P^{(i-1)}K$ where $Z_{i-1} = [\tilde{Z}_{i-1}, \tilde{Z}_{i-2}, \cdots, \tilde{Z}_1]$, show that $P_i \tilde{K}_{i-1} = P^{(i)}K$ where $Z_i = [\tilde{Z}_i, Z_{i-1}]$, $Z_{i-1} \in \mathbb{R}^{n \times l(i-1)}$, $\tilde{Z}_i \in \mathbb{R}^{n \times l_i}$ and $l = \sum_{r=i}^{i} l_i$.

$\square$

Recursive deflation: 1D example

Poisson equation,

$$
\begin{aligned}
-\frac{d}{dx}\left(c(x)\frac{du(x)}{dx}\right) &= f(x), \quad x \in [0, l] \\
u(0) &= 0, \quad \frac{du}{dx}(l) = 0
\end{aligned}
$$

Recursive deflation: 1D example

Introduce a FE mesh for the line $[0, l]$ including 3 domains $\Omega_1 = \{x_1, .., x_4\}$, $\Omega_2 = \{x_5, .., x_8\}$ and $\Omega_3 = \{x_9, .., x_{13}\}$. For sake of simplicity we will write $c_i = c(x_i)$ where $i = 1, ..., 13$, $x_1 = h$ and $x_{13} = l$. Furthermore because c_i is constant on each material domain we will use $c_i = c_1$, $c_i = c_2$ and $c_i = c_3$ on Ω_1, Ω_2 and Ω_3 respectively.

Recursive deflation: 1D example

After discretization,

$$K = \frac{1}{h}\begin{bmatrix}
2c_1 & -c_1 & & & & & & & & \\
-c_1 & \ddots & \ddots & & & & & \emptyset & & \\
 & \ddots & 2c_1 & -c_1 & & & & & & \\
 & & -c_1 & c_1 + c_2 & -c_2 & & & & & \\
 & & & -c_2 & \ddots & \ddots & & & & \\
 & & & & \ddots & 2c_2 & -c_2 & & & \\
 & & & & & -c_2 & c_2 + c_3 & -c_3 & & \\
 & & & & & & -c_3 & \ddots & \ddots & \\
 & \emptyset & & & & & & \ddots & 2c_3 & -c_3 \\
 & & & & & & & & -c_3 & c_3
\end{bmatrix}$$

Recursive deflation: 1D example

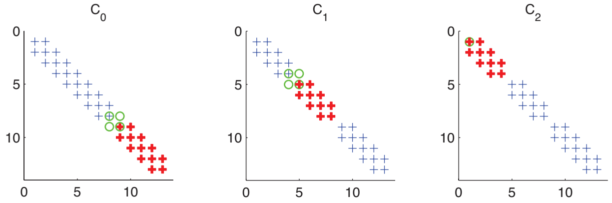

Figure: sparsity pattern C_0, C_1 and C_2. Nonzero elements represented by symbols; corresponding to deflated material, interface elements and remaining elements pictured by bold crosses, circles and non bold crosses respectively.

Recursive deflation: 1D example

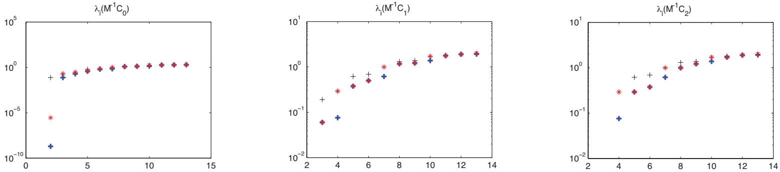

Figure: spectrum of $M^{-1}C_i$ ($\star$ correct, $+$ wrong choice deflation vectors) compared to spectrum of $M^{-1}K$ ($+$)

Numerical experiment: real asphalt core

Consider picture from introduction. Size of system approx. 3 million DOF, material parameters given in table below,

Table:

(a) E modulus materials

aggregate	bitumen	air voids
70000	5000	100

Numerical experiment: real asphalt core

We compare PCG and DPCG combined with three different preconditioners,

- diagonal scaling: low cost, weak properties
- AMG smoothed aggregation, default parameters, no specific information on mesh provided: relative low set up and solve cost, designed for solving elastic equations
- AMG smoothed aggregation, approx. null space of operator and dof-to-node mapping provided: expensive set up and solve cost, high memory usage

Numerical experiment: real asphalt core

	4 CPUs	8 CPUs	64 CPUs	iterations
PCG - diag	nc	nc	nc	nc
DPCG - diag	9883	5456	**680**	9018
PCG - SA	6687	6906	1123	2018
DPCG - SA	9450	5043	771	1210
PCG - SA^+	oom	2200	oom	407

Numerical experiment: real asphalt core

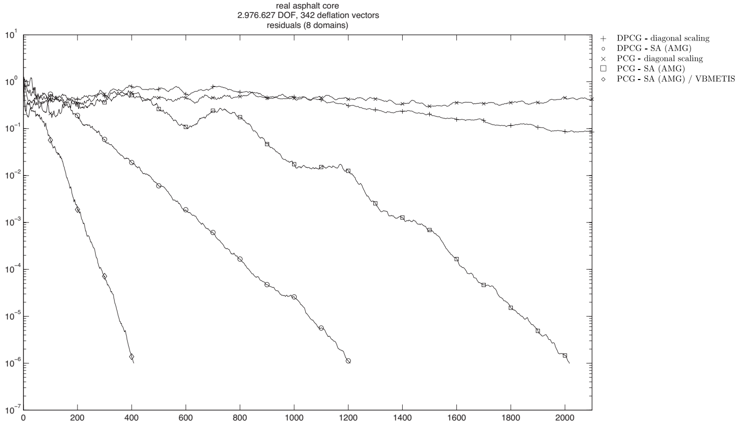

Figure: numerical results: residuals

Numerical experiment: real asphalt core

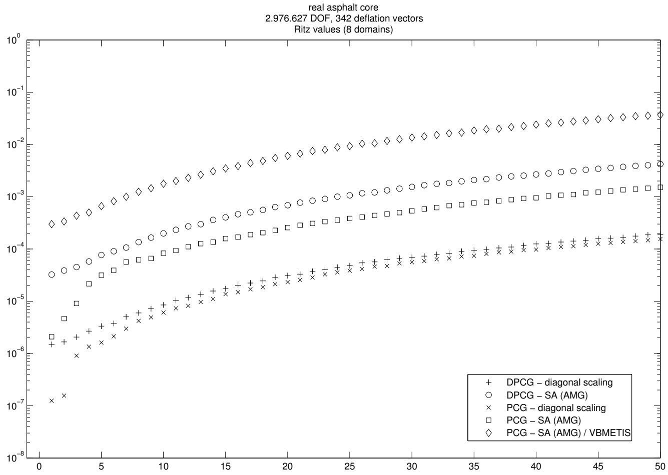

Figure: numerical results: Ritz values derived from (D)PCG

Questions and references

J. Frank and C. Vuik.
On the construction of deflation-based preconditioners.
SIAM J. Sci. Comput., 23(2):442–462, 2001.

T.B. Jönsthövel, M.B. van Gijzen, C.Vuik, C. Kasbergen, and A. Scarpas.
Preconditioned conjugate gradient method enhanced by deflation of rigid body modes applied to composite materials.
Computer Modeling in Engineering and Sciences, 47:97–118, 2009.